

PLASMA HYDROGENATION OF HYDROTHERMALLY GROWN ZNO MICROPODS

¹Zdeněk REMEŠ, ²Kateřina AUBRECHTOVÁ DRAGONOVÁ, ³Julia MIČOVÁ

¹FZÚ- Institute of Physics, Czech Academy of Sciences, Praha, Czech Republic, EU, remes@fzu.cz

²FZÚ- Institute of Physics, Czech Academy of Sciences, Praha, Czech Republic, EU, dragounova@fzu.cz

³Institute of Chemistry, Slovak Academy of Sciences, Bratislava, Slovakia, EU, chemjumi@savba.sk

<https://doi.org/10.37904/nanocon.2020.3777>

Abstract

The hydrothermally grown ZnO micropods have been placed on grounded stainless-steel holder and exposed to an inductively coupled plasma (ICP) monitored in-situ by optical emission spectroscopy (OES). OES shows the immediate release of oxygen during Ar ion bombardment. The prolonged exposure to hydrogen plasma leads to deterioration of the optical properties as well. The exposure, rf power and hydrogen pressure have been optimized to enhance UV-photoluminescence peak at the wavelength 384 nm related to surface bounded excitons and reduce the defect-related photoluminescence in red spectral range. The strong UV photoluminescence appears just after 1 minute of plasma hydrogenation in a radio frequency plasma discharge with power density 40 W/dm³ and hydrogen pressure 17 Pa.

Keywords: ZnO, micropods, inductively coupled plasma, optical emission spectroscopy, photoluminescence spectroscopy, Raman spectroscopy, infrared absorption spectroscopy

1. INTRODUCTION

The zinc oxide (ZnO) crystallite powder is a low cost, environmentally friendly, wide band gap semiconducting material with unique optical properties and variety of nanoparticle (NPs) morphologies [1]. Due to the high surface-to-volume ratio and related size effects, ZnO NPs are used in many applications for energy conversion, photocatalytic wastewater treatment, electrochemical energy storage or sensing. Recently, we have applied a hydrothermal chemical synthesis as a low-cost technology for mass-production of ZnO hedgehog-like crystallite powder [2], studied their crystal quality [3] and shown that the age of precursors plays a significant role in defect formation [4]. The photoluminescence spectra (PLS) show a strong near UV emission peak related to bound exciton complexes assigned to surface states [5]. The strong correlation between surface defects and the exciton emission has been also observed in hydrothermally synthesized ZnO micropods [6].

Particularly important are electrically conductive ZnO NPs with the interstitial hydrogen acting as a donor [7]. Two-step annealing in air at around 1000 °C followed by annealing in hydrogen atmosphere at 800 °C has been demonstrated to significantly enhance UV-photoluminescence of ZnO NPs for highly efficient sub-nanosecond fast scintillators [8,9]. The inductively coupled plasma (ICP) offers an alternative way of cold hydrogenation [10]. We have already shown that the cold hydrogenation in low pressure hydrogen plasma is an effective way to significantly enhance the electrical conductivity and exciton-related emission in ZnO thin films prepared by reactive magnetron sputtering on fused silica glass substrates [11]. In this paper we optimize the plasma hydrogenation of ZnO micropods placed on grounded stainless-steel sample holder.

2. EXPERIMENTAL

2.1. Hydrothermal growth

ZnO micropods were hydrothermally synthesized in aqueous solution containing equimolar (25 mM) amount of zinc nitrate hexahydrate p.a. ($\text{Zn}(\text{NO}_3)_2 \cdot 6\text{H}_2\text{O}$) and hexamethylenetetramine (HMTA) ($\text{C}_6\text{H}_{12}\text{N}_4$) p.a. Both chemicals were purchased from Slavus and used without further purification. Deionized water was purified with a system So~Safe Water Technologies, having a conductivity $0.20 \mu\text{S} \cdot \text{cm}^{-1}$ (25 °C). The reaction mixture was heated at 90 °C for 3 h. The precursor salt residues were removed from the sample by washing 5-times with deionized water followed by centrifugation at 10 000 rpm (RCF: 11 510g) for 15 min. Finally, the ZnO powder was dried by lyophilization. Scanning electron microscopy (SEM) images show ZnO micropods with hexagonal shape, the length up to 10 μm and the diameter about 0.5 μm , see **Figure 1**.

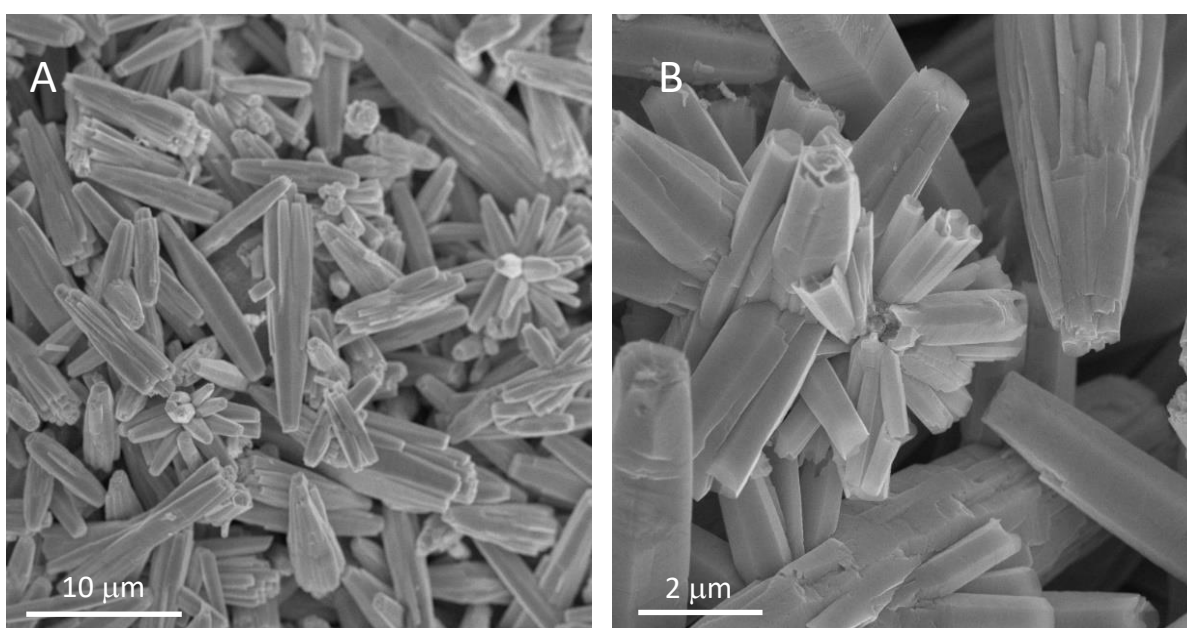


Figure 1 SEM images of hydrothermally grown ZnO micropods taken by MAIA3 (TESCAN) using the electron beam energy 5 keV (A) and 20 keV (B)

2.2. Plasma treatment

The plasma hydrogenation has been done in a prototype inductively coupled plasma (ICP) reactor currently being developed in a cooperation with the Czech company SVCS Process Innovation, s. r. o. (Valašské Meziříčí, Czech Republic). The quartz reactor of the active volume 5 liters operates at radio frequency (rf) 13.56 MHz with maximum discharge power up to 300 W corresponding to the power density $60 \text{ W}/\text{dm}^3$. The setup is evacuated with the Agilent Triscroll 300 dry vacuum pump protected with the ISO Flange Vacuum Filter (CSL-843-NW25). A 5 mg powder sample mechanically pressed into a round pellet with the diameter 3 mm was placed in the middle of the chamber on a grounded stainless-steel holder. The holder grounding is a recent improvement over the previously used ungrounded quartz holder. Prior the plasma treatment, the chamber, valves, flowmeters, gauges and all gas inlet and outlet tubes were evacuated to residual pressure below 0.1 Pa and flushed 5 min by 20 sccm flow of process gases to reduce residual gas contamination. The pellets were exposed for 30 s to Ar plasma (Ar purity 99.998%, rf power 100 W, Ar flow 5 sccm, pressure 16 Pa) followed by up to 20 min of hydrogen plasma exposure (H_2 purity 99.999%, rf power 200 W, H_2 flow 20 sccm, pressure 17 Pa). The originally white ZnO pellets became darker after prolonged plasma hydrogenation, see **Figure 2**.

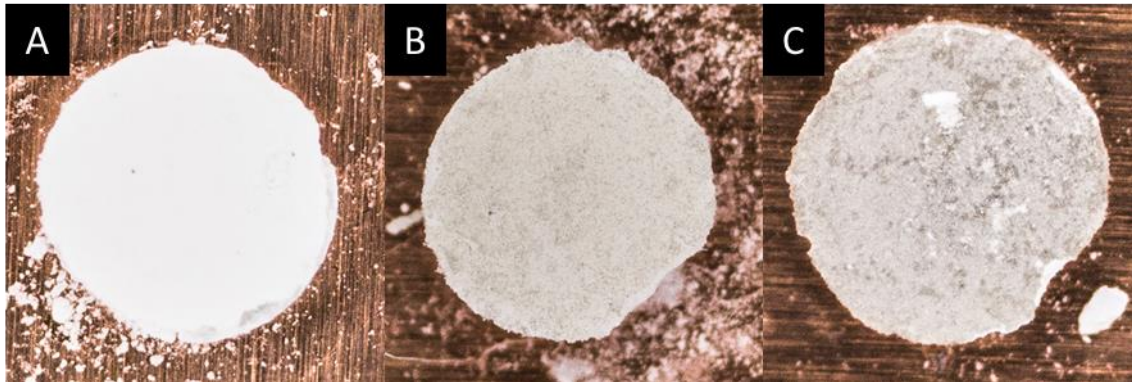


Figure 2 Optical images of ZnO pellets (diameter 3 mm) after 2 min (A), 10 min (B) and 20 min (C) plasma hydrogenation taken with a macro objective (Lumix G Macro 30 mm, F2.8 ASPH).

2.3. Characterization

Optical emission spectra (OES) were measured in 400-1000 nm spectral range with 1 nm spectral resolution by spectrally calibrated fiber coupled CCD spectrometer (B&W Tek BTC112E) focused in the middle of the quartz chamber. Dark spectra were subtracted. The integration time varied from 5 ms for Ar plasma to 200 ms for H₂ plasma. Each spectrum was averaged 10 times.

Raman spectra were recorded in backscatter geometry using a micro-spectroscopic Renishaw InVia Reflex Raman setup with integrated optical microscope and a charge-coupled device (CCD) camera. For excitation, a 442-nm-line of HeCd excitation laser. Other parameters were 100× Olympus objective, 65 μm slits, and a grating of 2400 grooves/mm.

The attenuated total reflectance (ATR) infrared absorption spectra were detected in 590-5000 cm⁻¹ spectral range and 4 cm⁻¹ resolution using Nicolet™ iS50 FTIR Spectrometer (Thermo Fisher Scientific) with build-in diamond ATR prism, KBr beam splitter and cooled DTGS detector. The ATR spectra were first normalized to zero at 5000 cm⁻¹ and then recalculated with the build-in advanced ATR correction for diamond prism.

PLS were measured at room temperature in the 360-780 nm spectral range with 2 nm spectral resolution using the 100 mW/cm² UV photo-excitation provided by a focused 340 nm LED equipped with a narrow band-pass filter and operating in square pulse regime at frequency 307 Hz. The emitted and scattered light was collected and focused onto the 1 mm wide input slit of double gratings SPEX 1672 monochromator equipped with Peltier cooled multi-dynode multi-alkali red sensitive photomultiplier (PMT) to be measured at each wavelength independently by a lock-in amplifier synchronized with excitation frequency. The spectra above 600 nm were measured with a long pass filter placed in front of the monochromator. The whole setup was spectrally calibrated with Oriel #63358 Quartz Tungsten halogen lamp and converted from wavelength to energy scale for quantitative analysis [12].

3. RESULTS AND DISCUSSION

The OES spectra clearly show the presence of atomic oxygen in Ar plasma as demonstrated by the presence of oxygen-related emission peaks at 777 and 845 nm [13], see **Figure 3**. Since no nitrogen related peaks are observed, oxygen cannot originate from ambient atmosphere leak, but from ZnO powder. In pure Ar plasma the intensity of O-peaks is low and may be explained by contamination from previously processed ZnO. The intensity of O-peaks increases by an order of magnitude when a pellet is placed into the chamber while the plasma visually change color from brownish to white. Thus, OES proves the heavy ion bombardment of the sample placed on grounded holder. Since only the Balmer series lines were observed in hydrogen plasma at 656, 486 and 434 nm and no O-peaks, we conclude that ZnO was scattered by heavy Ar ions but not by light H ions.

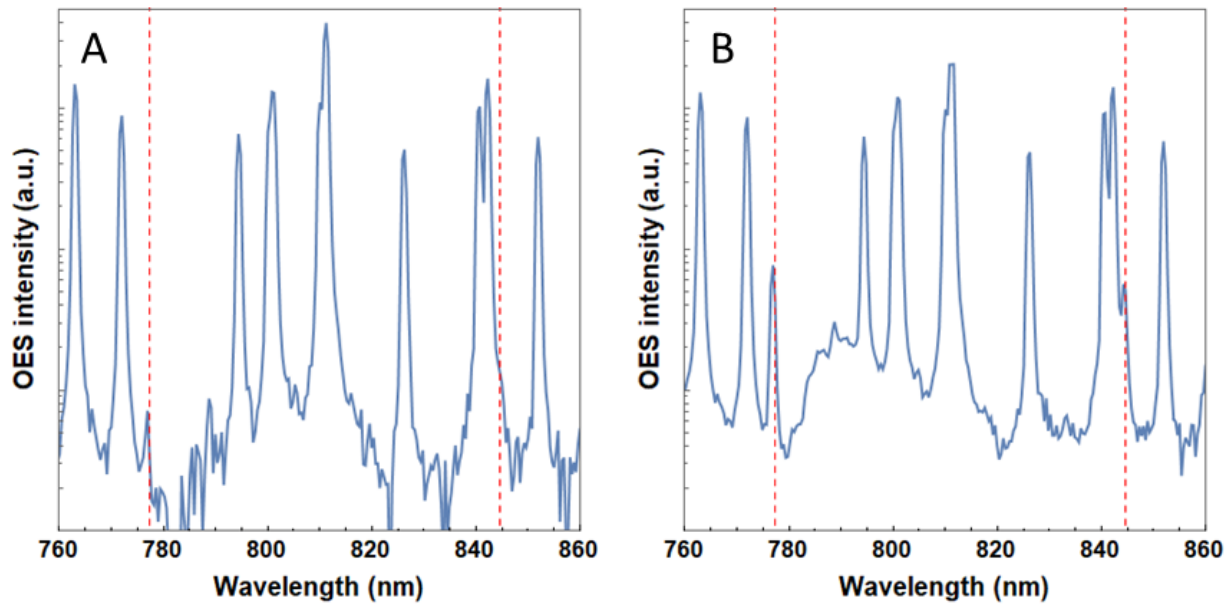


Figure 3 The semilogarithmic optical emission spectra of Ar plasma without (A) and with (B) ZnO pellet placed onto grounded stainless steel holder in the ICP reactor. The position of oxygen emission lines at 777 and 845 nm is indicated by dashed red lines.

Figure 4 (A) shows Raman spectra of plasma hydrogenated ZnO micropods, where origin of peaks is also depicted. Nonpolar phonon mode $E_2(\text{Low})$ expected at 100 cm^{-1} is associated with Zn sublattice, but it was out of the measured spectral range. Nonpolar phonon mode $E_2(\text{High})$ associated with oxygen sublattice is observed at 440 cm^{-1} [14]. The sharp, strong and dominant Raman peak is significantly amplified after hydrogen plasma, but for 10-minutes hydrogenation and longer its intensity decreases again. Same as increasing intensity of the dominant peak, broad sideband at low-frequency side also increases. This broad band with maximum about 420 cm^{-1} is attributed to $E_1(\text{TO})$ mode commonly seen in nano- and microstructures. The peaks at 336 and 540 cm^{-1} correspond to the sum and differential wavenumbers $E_2(\text{High}) \pm E_2(\text{Low})$ and $A_1(\text{LO})$, respectively [15]. The peak at 581 cm^{-1} has been assigned to the ZnO mode $E_1(\text{LO})$ [16]. This mode should be inactive but it may appear as a local mode due to the disturbance of the crystal symmetry resulting from the presence of oxygen vacancies and zinc interstitials. Thus, the presence of this mode suggests that the plasma treatment increases the concentration of point defects. Moreover, from spectra normalized on the value of $E_2(\text{High})$ peak, see **Figure 4(B)**, could be seen that for hydrogenation time up to 5 minutes, the spectra are very similar. After longer hydrogenation, the height of the $E_1(\text{LO})$ peak decreases. In spectra, small band near 660 cm^{-1} and 1150 cm^{-1} correspond to multiphonon processes and peak near 1100 cm^{-1} to combination of acoustic modes with symmetry A_1 and E_2 .

ATR-FTIR is a sensitive probe of free carriers in ZnO. It has been shown that the room-temperature exposure of polycrystalline ZnO films to H_2 plasma rapidly increases carrier density [17]. **Figure 5** shows the infrared absorbance spectra of plasma hydrogenated ZnO micropods depending on the expose to hydrogen plasma. Free carrier absorption dominates infrared absorbance spectra already in the unhydrogenated sample with further increase after plasma hydrogenation. The room temperature plasma hydrogenation had been sufficient to induce significant surface conductivity changes after 1 minute expose. It should be noted that the absorbance has been somewhat arbitrary normalized to zero at 5000 cm^{-1} and that the signal-to-noise ratio is poor in the spectral range $2000\text{-}2300\text{ cm}^{-1}$ where diamond ATR prism heavily absorbs.

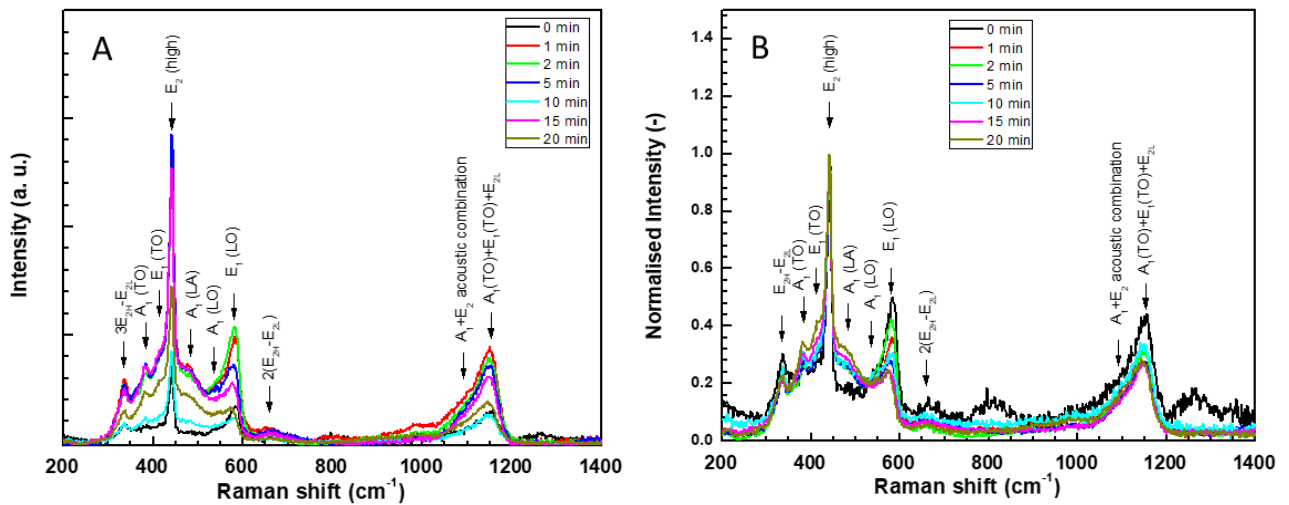


Figure 4 Raman spectra (A) and normalized Raman spectra (B) of plasma hydrogenated ZnO micropods depending on the expose to hydrogen plasma. The excitation wavelength was 442 nm (blue laser)

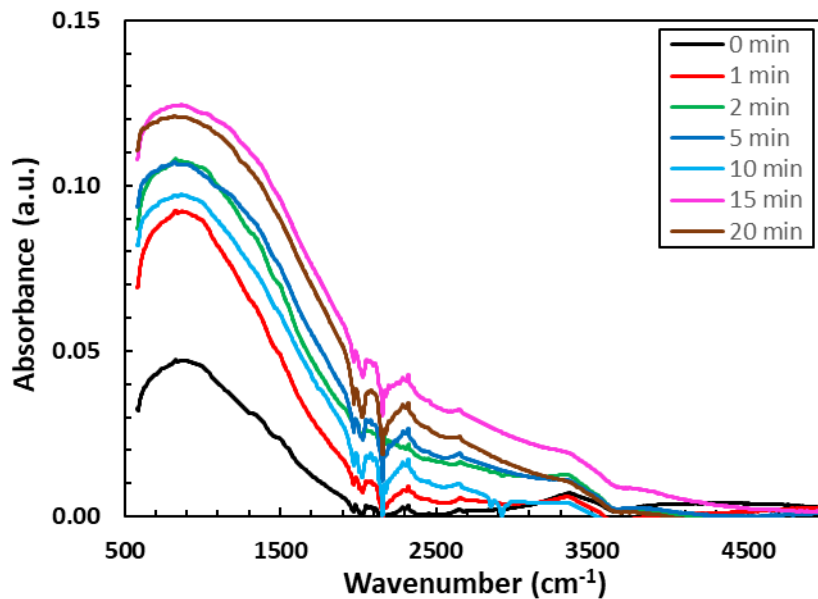


Figure 5 Infrared absorbance spectra of plasma hydrogenated ZnO micropods depending on the expose to hydrogen plasma measured by ATR FTIR and normalized to zero at 5000 cm^{-1} .

The PLS in **Figure 6** shows that the strong exciton photoluminescence at 3.23 eV (384 nm) appears already after 1 min plasma hydrogenation at 200 W. This suggest that the bound exciton complexes are assigned to surface states. Furthermore, the hydrogen plasma suppresses the defect related broad PLS band centered in red spectra range around 2 eV. It takes about 10 min to suppress this band by an order of magnitude. Therefore, we suggest 5 min plasma hydrogenation as an optimal process time. This is significantly shorter time then 30 min previously used in plasma hydrogenation with ungrounded quartz holder.

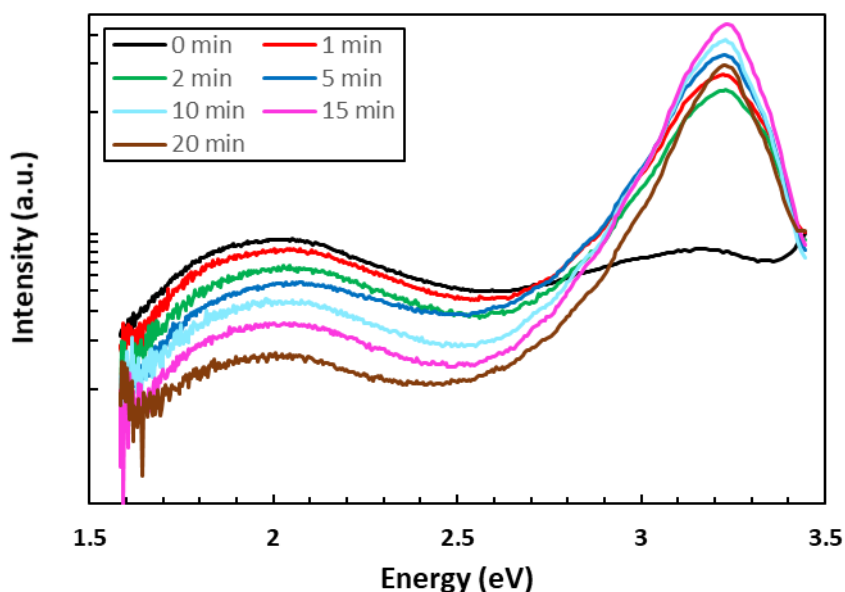


Figure 6 The room temperature PLS of plasma hydrogenated ZnO micropods in semilogarithmic intensity scale depending on the expose to hydrogen plasma. The excitation energy was 3.65 eV.

4. CONCLUSION

Ar plasma sputters ZnO placed on a grounded stainless-steel holder in an ICP reactor. Therefore, the Ar cleaning process needs to be taken only for a short time with a relatively low rf power. The strong UV photoluminescence appears just after a minute of plasma hydrogenation of ZnO micropods which is a strong evidence that the bound exciton complexes are assigned to surface states. On the other hand, the reduction of red photoluminescence needs prolonged time suggesting that the red photoluminescence is related to bulk defect states. The optimal time for plasma hydrogenation at the rf power density 40 W/dm³ and hydrogen pressure 17 Pa seems to be just a few minutes.

ACKNOWLEDGEMENTS

This work was supported by the Czech Science Foundation project 19-02858J, by the Operational Programme Research, Development and Education project SOLID21 - CZ.02.1.01/0.0/0.0/16_019/0000760 and by the Scientific Grant Agency of Ministry of Education, Science, Research and Sport of Slovak Republic and Slovak Academy of Sciences (VEGA 2/0157/20). Special thanks to Ing. Rayisa Yatskiv from the Institute of Physics of the Czech Academy of Sciences for SEM.

REFERENCES

- [1] KLINGSHIRN, C. F. (ed.). *Zinc Oxide: from fundamental properties towards novel applications*. Heidelberg ; London : Springer, 2010. Springer series in materials science, 120. ISBN 978-3-642-10576-0. QD181.Z6 Z56 2010.
- [2] CHANG, Yu-Ying, REMES, Zdenek, MICOVA, Julia. Mass production of hydrogenated ZnO nanorods. In : *NANOCON 2019 - Conference Proceedings* [online]. Hotel Voronez I, Brno, Czech Republic:Tanger Ltd., 2020. pp. 221–225. [Accessed 11 May 2020]. ISBN 978-80-87294-95-6. Available from: <https://www.confer.cz/nanocon2019-8680-chang-mass-production-of-hydrogenated-zno-nanorods.pdf>
- [3] MIČOVÁ, Júlia, BURYI, Maksym, ŠIMEK, Daniel, DRAHOKOUPIL, Jan, NEYKOVA, Neda, CHANG, Yu-Ying, REMEŠ, Zdeněk, POP-GEORGIEVSKI, Ognen, SVOBODA, Jan, IM, Chan. Synthesis of zinc oxide

- nanostructures and comparison of their crystal quality. *Applied Surface Science*. December 2018, vol. 461, pp. 190–195. DOI: 10.1016/j.apsusc.2018.05.176.
- [4] BURYI, M., BABIN, V., CHANG, Y.-Y., REMEŠ, Z., MIČOVÁ, J., ŠIMEK, D. Influence of precursor age on defect states in ZnO nanorods. *Applied Surface Science*. September 2020, vol. 525, p. 146448. DOI: 10.1016/j.apsusc.2020.146448.
- [5] FALLERT, Johannes, HAUSCHILD, Robert, STELZL, Felix, URBAN, Alex, WISSINGER, Markus, ZHOU, Huijuan, KLINGSHIRN, Claus, KALT, Heinz. Surface-state related luminescence in ZnO nanocrystals. *Journal of Applied Physics*. April 2007, vol. 101, no. 7, p. 073506. DOI: 10.1063/1.2718290.
- [6] GOKARNA, Anisha, AAD, Roy, ZHOU, Junze, NOMENYO, Komla, LUSSON, Alain, MISKA, Patrice, LERONDEL, Gilles. On the origin of the enhancement of defect related visible emission in annealed ZnO micropods. *Journal of Applied Physics*. 14 October 2019, vol. 126, no. 14, p. 145104. DOI: 10.1063/1.5111184.
- [7] VAN DE WALLE, Chris G., NEUGEBAUER, J. Universal alignment of hydrogen levels in semiconductors, insulators and solutions. *Nature*. June 2003, vol. 423, no. 6940, pp. 626–628. DOI: 10.1038/nature01665.
- [8] BOURRET-COURCHESNE, E.D., DERENZO, S.E., WEBER, M.J. Development of ZnO:Ga as an ultra-fast scintillator. *Nuclear Instruments and Methods in Physics Research Section A: Accelerators, Spectrometers, Detectors and Associated Equipment*. April 2009, vol. 601, no. 3, pp. 358–363. DOI: 10.1016/j.nima.2008.12.206.
- [9] [PROCHÁZKOVÁ, Lenka, GBUR, Tomáš, ČUBA, Václav, JARÝ, Vítězslav, NIKL, Martin. Fabrication of highly efficient ZnO nanoscintillators. *Optical Materials*. September 2015, vol. 47, pp. 67–71. DOI: 10.1016/j.optmat.2015.07.001.
- [10] GRILL, Alfred. *Cold plasma in material fabrication: from fundamentals to applications*. New York: The Institute of Electrical and Electronics Engineers, Inc., 1994. ISBN 0-7803-4714-5.
- [11] CHANG, Y.-Y., NEYKOVA, N., STUHLIK, J., PURKRT, A., REMES, Z. Hydrogen plasma treatment of ZnO thin films. In: *NANOCON 2016 - Conference Proceedings*. Ostrava, Czech Republic: TANGER Ltd., 2016. pp. 161–165. ISBN 978-80-87294-71-0.
- [12] MOONEY, Jonathan, KAMBHAMPATI, Patanjali. Get the Basics Right: Jacobian Conversion of Wavelength and Energy Scales for Quantitative Analysis of Emission Spectra. *The Journal of Physical Chemistry Letters*. 3 October 2013, vol. 4, no. 19, pp. 3316–3318. DOI: 10.1021/jz401508t.
- [13] KRAMIDA, Alexander, RALCHENKO, Yuri. NIST Atomic Spectra Database, NIST Standard Reference Database 78 [online]. 1999. National Institute of Standards and Technology. [Accessed 25 August 2020]. Available from: <http://www.nist.gov/pml/data/asd.cfm>.
- [14] YANG, J. H., ZHENG, J. H., ZHAI, H. J., YANG, L. L. Low temperature hydrothermal growth and optical properties of ZnO nanorods. *Crystal Research and Technology*. January 2009, vol. 44, no. 1, pp. 87–91. DOI: 10.1002/crat.200800294.
- [15] CALLEJA, J. M., CARDONA, Manuel. Resonant Raman scattering in ZnO. *Physical Review B*. 15 October 1977, vol. 16, no. 8, pp. 3753–3761. DOI: 10.1103/PhysRevB.16.3753.
- [16] DECREMPS, Frédéric, PELLICER-PORRES, Julio, SAITTA, A. Marco, CHERVIN, Jean-Claude, POLIAN, Alain. High-pressure Raman spectroscopy study of wurtzite ZnO. *Physical Review B* [online]. 6 February 2002, vol. 65, no. 9. [Accessed 29 February 2020]. DOI: 10.1103/PhysRevB.65.092101. Available from: <https://link.aps.org/doi/10.1103/PhysRevB.65.092101>.
- [17] WOLDEN, C.A., BARNES, T.M., BAXTER, J.B., AYDIL, E.S. Infrared detection of hydrogen-generated free carriers in polycrystalline ZnO thin films. *Journal of Applied Physics* [online]. 2005, vol. 97, no. 4. DOI: 10.1063/1.1851599.